DOI 10.1007/s11182-017-1210-8

Russian Physics Journal, Vol. 60, No. 8, December, 2017 (Russian Original No. 8, August, 2017)

NUMERICAL MODELING OF ULTRA WIDEBAND COMBINED ANTENNAS

M. Yu. Zorkal'tseva, V. I. Koshelev, and A. A. Petkun UDC 621.373

With the help of a program we developed, based on the finite difference method in the time domain, we have investigated the characteristics of ultra wideband combined antennas in detail. The antennas were developed to radiate bipolar pulses with durations in the range 0.5–3 ns. Data obtained by numerical modeling are compared with the data of experimental studies on antennas and have been used in the synthesis of electromagnetic pulses with maximum field strength.

Keywords: combined antenna, radiation center, synthesis of electromagnetic pulses.

INTRODUCTION

Three-dimensional KA combined antennas [1], such as those developed at the Institute of High-Current Electronics, are in wide use at the present time [2, 3]. Broadening of the operating frequency band in such antennas is achieved thanks to a combination of radiators of electric and magnetic type, providing a reduction of the reactive energy in the near zone of the antenna and, as a consequence, constancy of the input impedance over a wider frequency range. At the present time, KAs exist which have been designed to radiate bipolar pulses of different durations τ_p = 0.5–3 ns [4–7]. Creation of an antenna array, where each antenna is optimized to radiate a bipolar pulse of prescribed duration, makes it possible to synthesize electromagnetic pulses with different characteristics. In other words, adding together pulses in different frequency ranges with matched time delays makes it possible to vary the frequency overlap coefficient $b_f = f_H/f_L$ of the amplitude spectrum, and also to vary the shape of the synthesized pulse and the peak field strength.

The characteristics of the given antennas were optimized [8] with the help of the computer program 4NEC2, based on the method of moments, and within the framework of the given approach the antenna surfaces were modeled by a set of piecewise-continuous thin wires. Maxwell's equations are solved numerically in the given program only in the frequency domain, which is acceptable for calculation of frequency dependences of the voltage standing-wave ratio (VSWR). However, the capabilities of the program do not permit one to obtain the directivity diagram (DD) of the antenna in the time domain. For numerical modeling of ultra wideband radiators, it would be advantageous to use the finite difference method in the time domain [9], which would make it possible to obtain the characteristics of the antenna in one calculation over a wide frequency range. For these purposes, we created a computer program which has been successfully applied to numerical modeling of three-dimensional spiral antennas [10].

The goal of this work was to develop a computer program module to import the geometries of antennas of complex shape, to investigate numerically the characteristics of KAs, excited by bipolar pulses of duration 0.5–3 ns, in the frequency and time domains, and also to synthesize radiation pulses with maximum peak electric strength.

Institute of High-Current Electronics of the Siberian Branch of the Russian Academy of Sciences, Tomsk, Russia, e-mail: fear2029@sibmail.com; koshelev@lhfe.hcei.tsc.ru; pit@lhfe.hcei.tsc.ru. Translated from Izvestiya Vysshikh Uchebnykh Zavedenii, Fizika, No. 8, pp. 26–30, August, 2017. Original article submitted June 29, 2017.

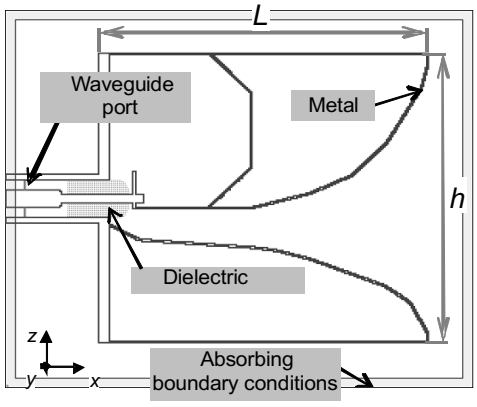

Fig. 1. Geometry of the calculational problem for obtaining the shape of the reflected voltage pulse of the KAs.

STATEMENT OF THE PROBLEM

The program we developed, based on the finite difference method in the time domain, includes a block of program modules and a graphic interface for specifying antenna geometries. To download KA geometries into the program for numerical modeling, we developed a module for importing geometries from a CAD file. This module allows one to download arbitrary surfaces of metallic and dielectric bodies with complex geometrical structure, which significantly broadens the capabilities of the program for numerical modeling purposes. The second part of the program includes a block of modules and a graphic interface for prescribing the mathematical model and its numerical realization. The program is based on a library developed earlier, containing a hierarchy of classes for solutions of problems of the electrodynamics of continuous media. In particular, the problem of numerical modeling of transmitting antennas includes: a realization of the finite difference method in the time domain, creation of excitation sources, and realization of an algorithm for extending the fields into the far zone and assigning the boundary conditions on the calculational domain. Figure 1 presents the geometry of the calculational problem for obtaining the shape of the reflected voltage pulse of the KA, used to calculate the VSWR. To calculate the time dependences of the fields in the far zone, we modeled only the surface of the antenna without the coaxial cable and the dielectric. The metallic surfaces in the model were assumed to be perfectly conducting. To control the shape of the reflected voltage pulse, we used a waveguide port as the excitation source. In some cross section of the coaxial line, the distribution of the radial component of the electric field E_ρ was assigned, together with its relation to the electric field components on a Cartesian grid with account of the displacements for E_x and E_y. In the calculation of the DD, we used a source with concentrated parameters in the form of a difference circuit for the E_z component of the electric field, allowing for a wave impedance of 50 Ω. The source was located between the back wall of the KA and the horizontal feed. The corresponding KAs were excited by bipolar pulses with durations equal to 0.5, 1, 2, and 3 ns at the 0.1 level. To obtain the time dependences of the components of the electric field in the far zone, the source and the antenna were enclosed by a closed Huygens surface. In this work, to calculate the fields, we used the Kirchhoff integral representation

$$\psi(\boldsymbol{r},t)=\frac{1}{4\pi}\oint_{S_{\mathrm{H}}}\boldsymbol{n}\left[\frac{\operatorname{grad}'\psi(\boldsymbol{r}',\tau_d)}{|\boldsymbol{r}-\boldsymbol{r}'|}-\frac{\boldsymbol{r}-\boldsymbol{r}'}{|\boldsymbol{r}-\boldsymbol{r}'|^3}\psi(\boldsymbol{r}',\tau_d)-\frac{\boldsymbol{r}-\boldsymbol{r}'}{c|\boldsymbol{r}-\boldsymbol{r}'|^2}\frac{\partial\psi(\boldsymbol{r}',\tau_d)}{\partial\tau_d}\right]ds'_{\mathrm{H}}, \quad (1)$$

where the scalar function $\psi(\boldsymbol{r}, t)$ corresponds to some component of the electric field, $\boldsymbol{n}$ is the outer normal to the Huygens surface S_{H}, $\boldsymbol{r}$ is the radius vector of a point in the far zone, $\boldsymbol{r}'$ is the radius vector of a point on the surface S_{H},

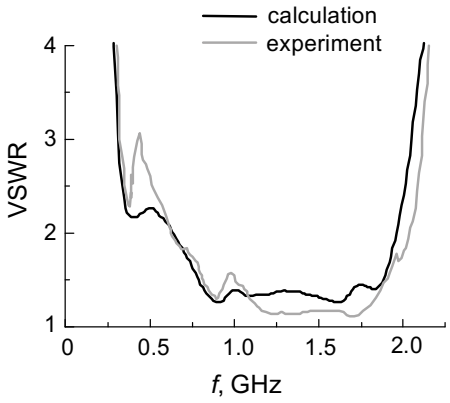

Fig. 2. Calculated dependence and experimental dependence of the VSWR for KA2.

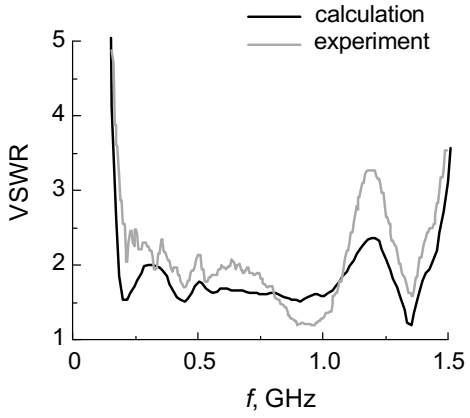

Fig. 3

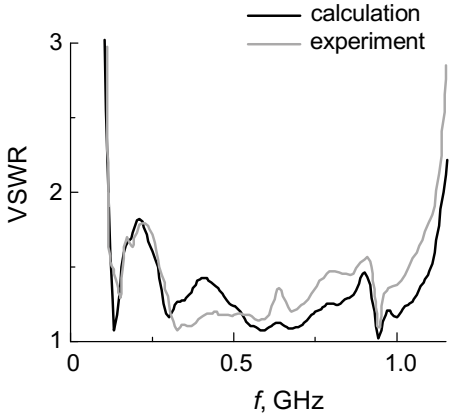

Fig. 4

Fig. 3. Calculated dependence and experimental dependence of the VSWR for KA3.

Fig. 4. Calculated dependence and experimental dependence of the VSWR for KA4.

c is the velocity of light in free space, and τ_d is the time delay for the fields, defined as $\tau_d = t - |\boldsymbol{r} - \boldsymbol{r}'|/c$ [11]. As boundary conditions, we used a Uniaxial Perfectly Matched (absorbing) Layer (UPML) with polynomial grading of the parameters [9].

We denote the KAs for radiation of bipolar pulses with durations 0.5, 1, 2, and 3 ns as KA1, KA2, KA3, and KA4, respectively. The spatial discretization steps were assigned as follows: $\Delta x = \Delta y = \Delta z = 1$ mm for KA1, $\Delta x = \Delta y = \Delta z = 1.5$ mm for KA2, and $\Delta x = \Delta y = \Delta z = 2$ mm for the other two variants. The time discretization step was chosen in accordance with the Courant condition for three-dimensional realization of the finite difference method in the time domain: $\Delta t \le \Delta x/\sqrt{3}\ /c$. The width and height of the KA corresponded to $h = 0.5\tau_p\, c$, and the length $L > h$.

NUMERICAL MODELING OF COMBINED ANTENNAS

Using the developed code, we calculated frequency dependences of the VSWR. For all of the antennas, good agreement with the experimental curves is observed. Figures 2, 3, and 4 plot the calculated and experimental frequency

TABLE 1. Radiation Center and Boundary of the Far Zone of the KA

Parameters	KA1	KA2	KA3	KA4
Radiation center, cm	7.2	13	24	35
Distance from the radiation center x_0 to the aperture of the KA, cm	1.8	4	8	12.6
Boundary of the far zone, cm	47.2	63	104	155

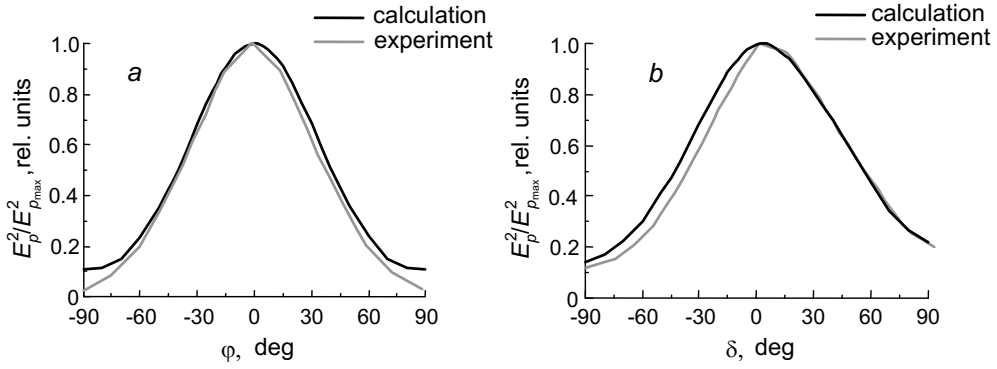

Fig. 5. Calculated and experimental DDs, normalized to the peak power, for the components of the electric field in the *H*-plane (*a*) and in the *E*-plane (*b*) for KA2.

dependences of the VSWR for KA2, KA3, and KA4, respectively. The frequency overlap coefficient b_f for the VSWR level ≤ 2 for KA1 was 3.5: $b_f = 3.5$, for KA2, it was 3.1, and for KA3 and KA4 the overlap coefficients were 5–8, and roughly 10, respectively.

The coordinate system for calculating the radiation characteristics was chosen as follows: the angle θ between the radius vector $\boldsymbol{r}$ of a point in the far zone and the *Oxy* plane (Fig. 1) was chosen such that $\delta = 90° - \theta$. Thus, the *E*-plane corresponded to the case where the azimuthal angle was equal to zero: $\varphi = 0°$ (reckoned from the positive direction of the *Ox* axis), and the elevation angle was varied within the limits $90° \le \delta \le 90°$, while the *H*-plane corresponded to the case of a fixed elevation angle $\delta = 0°$ and variable azimuthal angle $-90° \le \varphi \le 90°$. The radiation characteristics were calculated using the Kirchhoff representation, where the center of the spherical coordinate system corresponded to the geometric center of the KA: $\boldsymbol{r}_c = (x_c, y_c, z_c) = (L/2, h/2, h/2)$, i.e., it was oriented in the direction δ, $\varphi = 0°$ and offset from the back wall of the KA by the distance $L/2$.

It was of interest to use the developed program to investigate the position of the radiation center of the antenna and the boundary of the far zone in the δ, $\varphi = 0°$ direction for excitation of bipolar pulses. It was assumed that the radiation center lies precisely on the δ, $\varphi = 0°$ axis. To find the radiation center, we used the criterion $(\boldsymbol{r} - \boldsymbol{r}_0)E_p(\boldsymbol{r}) \approx \text{const}$, where E_p is the peak electric field strength at the distance $|\boldsymbol{r}|$ and $\boldsymbol{r}_0$ is the radius vector of a reference point. We call that reference point the radiation center, for which we obtain the minimum distance to the boundary of the far zone. Distances along the antenna axis were measured from the back wall of the KA. Since it was assumed that the radiation center lies on the axis, we replace $\boldsymbol{r}$ by x, and $\boldsymbol{r}_0$ by x_0. Table 1 lists the positions of the radiation center and the boundaries of the far zone for the E_y-component of the electric field in the *H*-plane for the four KAs investigated.

With the help of the developed program, we obtained DDs in the *H*- and *E*-planes for all the KAs. Figures 5*a* and *b* present graphs of the calculated and experimental DDs, normalized to the peak power for KA2 in the *H*- and *E*-planes, respectively. Good agreement between the calculated and experimental DDs is observed.

Figures 6, 7, and 8 present graphs of the peak-power normalized DDs in the *H*- and *E*-planes for KA1, KA2, and KA3, respectively. In the *H*-plane the DDs are symmetric about the direction δ, $\varphi = 0°$. This is explained by the symmetry of the antenna with respect to the *Oxz* plane (see Fig. 1). In the *E*-plane, an asymmetry is observed since the

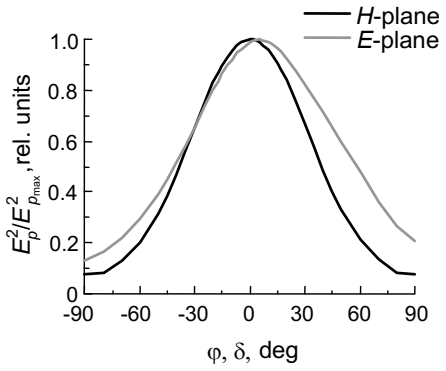

Fig. 6

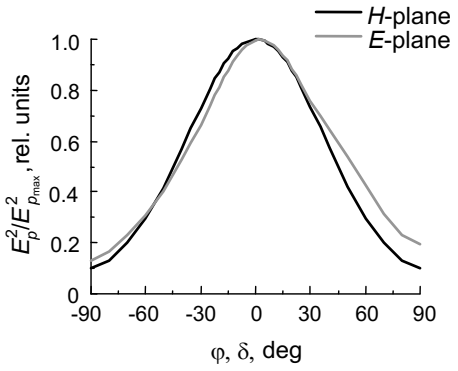

Fig. 7

Fig. 6. Calculated DDs, normalized to the peak power, in the *H*- and *E*-planes for KA1.

Fig. 7. Calculated DDs, normalized to the peak power, in the *H*- and *E*-planes for KA3.

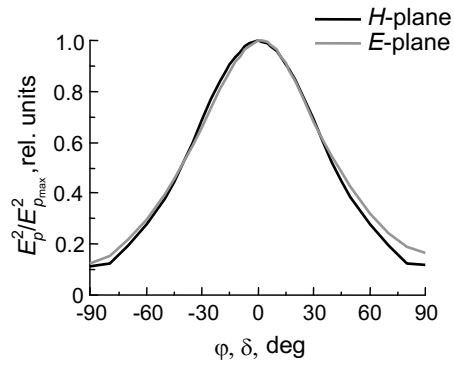

Fig. 8

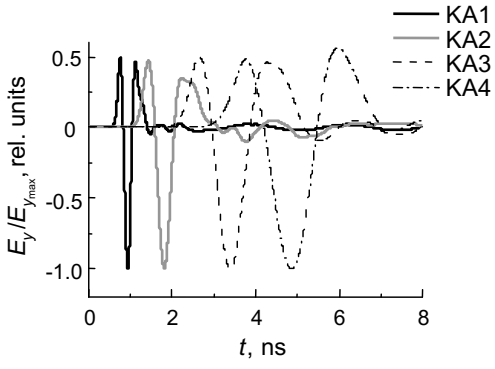

Fig. 9

Fig. 8. Calculated DDs, normalized to the peak power, in the *H*- and *E*-planes for KA4.

Fig. 9. Time dependence of the electric field component in the *H*-plane for KA1, KA2, KA3, and KA4 in the δ, φ = 0° direction.

antennas are not symmetric with respect to the *Oxy* plane. This asymmetry is most pronounced for KA1 and decreases with increase of the duration of the exciting bipolar pulse. For KA4, this asymmetry is weakly manifested.

Figure 9 plots the time dependence of the component of the electric field in the *H*-plane, obtained at a distance of 3 m from the center of the spherical coordinate system in the δ, φ = 0° direction for all four KAs. For all of the pulses, except the KA4 pulse, a distortion of the third lobe is observed resulting from frequency dispersion.

Figure 10 presents the result of a summation of the pulses shown in Fig. 9 for synchronization of the amplitude maximum, and Fig. 11 presents the amplitude spectrum of a synthesized pulse and amplitude spectra of the pulses of the four KAs. The overlap coefficient at the –10 dB level of the spectrum of the synthesized pulse was equal to 6.2: $b_f = 6.2$.

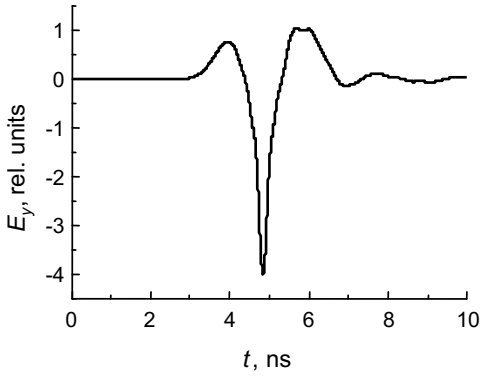

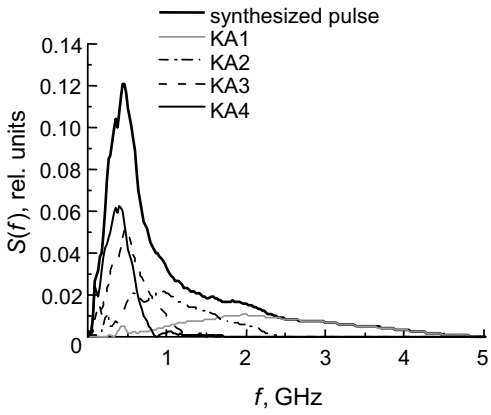

Fig. 10

Fig. 11

Fig. 10. Result of summation of the pulses radiated by KA1, KA2, KA3, and KA4, synchronized with reference to the maximum of the amplitude.

Fig. 11. Amplitude spectra of the synthesized pulse and pulses radiated by KA1, KA2, KA3, and KA4.

CONCLUSIONS

A module has been developed for importing bodies with complex geometrical structure from CAD files into a numerical modeling program. The given module has broadened the capabilities of the program. With its help, we have obtained characteristics of KAs optimized to radiate bipolar pulses with durations of 0.5, 1, 2, and 3 ns. The results obtained in the frequency and time domains are in good agreement with experiment. The calculated KA radiation pulses were used to synthesize an electromagnetic pulse with maximum peak field strength. In the calculations, we used the temporal shape and the spectrum of the synthesized pulse.

The authors thank V. V. Plisko for providing files containing KA geometries.

This work was partially supported by a grant from the Russian Scientific Foundation under Project No. 16-19-10081.

REFERENCES

1. Yu. A. Andreev, Yu. I. Buyanov, and V. I. Koshelev, Radiotekh. Elektron., **50**, No. 5, 585–594 (2005).
2. A. Mehrdadian and K. Forooraghi, Prog. Electromagn. Res. C, **39**, 37–48 (2013).
3. B. Cadilhon, B. Cassany, P. Modin, *et al*., Ultra Wideband Communications: Novel Trends – Antennas and Propagation, Chapter 15: Ultra Wideband Antennas for High Pulsed Power Applications, ed. M. Matin, InTech (2011); DOI: 10.5772/20305.
4. A. M. Efremov, V. I. Koshelev, B. M. Koval'chuk, *et al*., Prib. Tekh. Eksp., No. 1, 77–83 (2011).
5. A. M. Efremov, V. I. Koshelev, B. M. Koval'chuk, *et al*., Radiotekh. Elektron., **52**, No. 7, 813– 821 (2007).
6. V. P. Gubanov, A. M. Efremov, V. I. Koshelev, *et al*., Prib. Tekh. Eksp., No. 3, 46–54 (2005).
7. Yu. A. Andreev, A. M. Efremov, V. I. Koshelev, *et al*., Prib. Tekh. Eksp., No. 6, 51–60 (2011).

8. V. P. Belichenko, Yu. I. Buyanov, and V. I. Koshelev, Ultra Wideband Pulsed Radio Systems [in Russian], ed. V. I. Koshelev, Nauka, Novosibirsk (2015).
9. A. Taflove and S. C. Hagness, Computational Electrodynamics: The Finite-Difference Time-Domain Method, Artech House, Boston (2000).
10. M. Yu. Zorkal'tseva, V. I. Koshelev, and A. A. Petkun, Izv. Vyssh. Uchebn. Zaved. Fiz., **56**, No. 8/2, 149–153 (2013).
11. O. M. Ramahi, IEEE Trans. Ant. Prop., **45**, No. 5, 753–759 (1997).